3236–3243 *Nucleic Acids Research, 1999, Vol. 27, No. 15*

Presence of a coordinated metal ion in a *trans*-acting antigenomic *delta* ribozyme

Daniel A. Lafontaine, Sirinart Ananvoranich and Jean-Pierre Perreault*

Département de Biochimie, Faculté de médecine, Université de Sherbrooke, Sherbrooke, Québec J1H 5N4, Canada

Received January 25, 1999; Revised May 14, 1999; Accepted June 14, 1999

ABSTRACT

We have investigated the cleavage induced by metal ions in an antigenomic form of a *trans*-acting *delta* ribozyme. A specific Mg^{2+}-induced cleavage at position G_{52} at the bottom of the P2 stem was observed to occur solely within catalytically active ribozyme–substrate complexes (i.e. those that performed the essential conformational transition step). Only the divalent cations which support catalytic activity permitted the detection of specific induced cleavages in this region. Using various mutant ribozymes and substrates, we demonstrated a correlation between enzymatic activity and the Mg^{2+}-induced cleavage pattern. We show that the efficiency of the coordination of the magnesium to its binding site is related to the nature of the base pair in the middle of the P1 stem (i.e. Rz_{23}-S_8). Together with additional evidence from nuclease probing experiments that indicates the occurrence of a structural rearrangement involving the bottom of the P2 stem upon formation of the P1 helix, these results show that an intimate relationship exists between the folding and the catalytic activity of the *delta* ribozyme.

INTRODUCTION

Hepatitis delta virus (HDV) possesses a single-stranded circular RNA genome of 1.7 kb which replicates through a double-rolling-circle mechanism in human cells (1,2). The minimal sequences required for the optimum self-cleavage of both antigenomic and genomic strands *in vitro* are 1 nt 5' and 84 nt 3' of the cleavage site (1). According to the pseudoknot model (3), the secondary structure of *delta* ribozyme consists of four stems (P1–P4), two internal loops (L3 and L4) and three single-stranded junctions referred to as the linker stems (J1/2, J1/4 and J4/2) (Fig. 1). An additional stem formed by 2 bp, namely P1.1, was observed in the crystal structure of a self-cleaved form of the genomic ribozyme (4). From self-cleaving sequences, *trans*-acting ribozymes in which one molecule possesses the substrate sequence and the other the catalytic property, have been developed (1). We engineered a ribozyme from the antigenomic HDV genome possessing some modified features in order to obtain a catalytic RNA of minimal length (57 nt, Fig. 1; 5). Briefly, the J1/2 junction has been removed, and the P4 stem–loop has been replaced by a shorter ultra-stable stem–loop derived from the UNCG family (6). Finally, the P2 stem has been elongated, and the sequence modified so as to begin with three guanosines to facilitate *in vitro* transcription. Under single-turnover conditions, this ribozyme cleaved a model substrate (11 nt in size, Fig. 1) with a rate constant of 0.32 min^{-1}, an apparent K_M of 9.9 nM and an apparent second order rate constant of 3×10^7 $min^{-1}M^{-1}$ (5).

According to the crystal structure of genomic *delta* ribozyme no tightly bound metal ion is located within the catalytic RNA. This results in a structure that appears to be stabilized entirely by nucleic acid interactions (4). However, a previous study of the antibiotic inhibition of *delta* ribozyme suggested that both neomycin and magnesium are likely to displace lead ion(s), raising the hypothesis that *delta* ribozymes do indeed possess metal ion coordination site(s) (7). Recently, it has been shown that hammerhead, hairpin and VS ribozymes do not require divalent metal ions for their catalytic activity, provided that mimics such as cobalt hexaamine or monovalent metal ions can support the cleavage ability (8). In contrast, *delta* ribozyme has an absolute requirement for the presence of divalent metal ions in order for self-cleavage to occur (8), clearly indicating that divalent metal ions play an indispensable role in folding and/or active site chemistry of this ribozyme.

The induced cleavage approach has been successfully used by many groups to elucidate metal ion binding sites (e.g. 9–12). This method is based on the fact that water molecules bound by metal ions can be substantially more acidic than free ones. If a metal ion is coordinated to other ligands, the pK_a of a bound water molecule can be affected and the resulting hydroxide ion is a potent nucleophile (11). Since divalent metal ions can interact electrostatically with the phosphate backbone of RNA, hydroxide ions bound to a metal ion participate in a huge number of reactions including the common transesterification reaction (13). In order for a metal ion to cleave an RNA backbone, a proton from the 2'-hydroxyl (2'-OH) of a ribose moiety must be removed by a hydroxide ion and a certain flexibility must exist in the region. As a consequence, not all bound metal ions cleave the RNA backbone. By increasing the pH to near the pK_a of a particular metal ion, the concentration of hydroxide ion is increased and more ribose 2'-OH protons are removed. Eventually, more of the metal ions bound to the RNA are able to cleave the phosphodiester backbone. In this report, we examined the cleavage patterns induced by magnesium ions in an antigenomic form of a *trans*-acting *delta* ribozyme. We report a specific Mg^{2+}-induced cleavage of *delta* ribozyme that occurs solely in conjunction with the formation of a P1 helix that has the potential to lead to an active ternary complex. The

*To whom correspondence should be addressed. Tel: +1 819 564 5310; Fax: +1 819 564 5340; Email: jperre01@courrier.usherb.ca

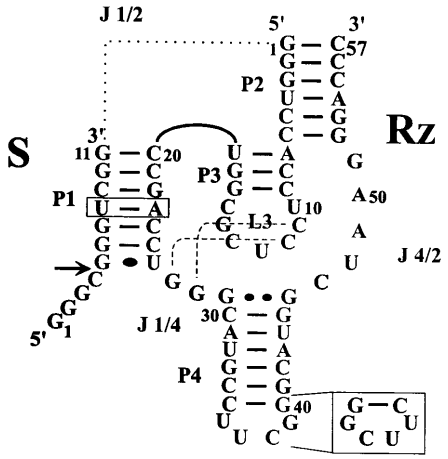

Figure 1. Secondary structure and nucleotide sequences of a *trans*-acting *delta* ribozyme. The base paired regions are numbered according to (3). The pseudoknot P1.1 (4), which is formed by $C_{11}C_{12}$ and $G_{27}G_{28}$, is illustrated by dashed lines. S and Rz represent substrate and ribozyme, respectively. The dotted line represents the J1/2 single-stranded region which joins the substrate and ribozyme molecules in the *cis*-form. The arrow indicates the cleavage site. The homopurine base pair at the top of the P4 stem is represented by two dots (G··G), while the wobble base pair is represented by a single dot (G·U).

presence of this metal ion coordinate site appears to be essential for the catalytic activity of the *delta* ribozyme.

MATERIALS AND METHODS

Materials

Restriction enzymes, nucleases, RNAGuard (RNase inhibitor), T4 polynucleotide kinase, Sephadex G-50 and [γ-^{32}P]ATP (6000 Ci/mmol) were obtained from Amersham Pharmacia Biotech. Yeast pyrophosphatase and calf intestine alkaline phosphatase were purchased from Roche Diagnostic. DNase I (RNase-free) was obtained from Promega. Magnesium chloride hexahydrate was purchased from Sigma-Aldrich. T7 RNA polymerase was purified as described using the expression system of Studier (14,15).

RNA synthesis

Plasmid carrying the delta ribozyme. The construction of the *trans*-acting *delta* ribozyme used in this work has been described previously (5,16; Fig. 1). Briefly, the construct was engineered as follows: two pairs of complementary overlapping oligonucleotides representing the entire length of the ribozyme (57 nt), were synthesized, annealed and ligated to *Hin*d*III*/*Sma*I codigested pUC19 yielding a plasmid harboring the *delta* ribozyme (referred to as pδRzP1.1; 16). pδRzP1.1 was then used for the construction of mutant ribozymes carrying the ultrastable tetraloop 4 (i.e. pδRzP1.1/P4.1) and the C_{47}A mutation (i.e. pδRzP1.1/P4.1/J4-2.1) as described previously (5). Ribozymes harboring mutations in the P1 region were constructed by modifying the substrate recognition site of pδRzP1.1 via ligation of an oligonucleotide containing the altered sequence flanked by the appropriate restriction endonuclease sites to *Rsr*II (U_{19})/*Sph*I (G_{33}) digested pδRzP1.1 (16,17). All ribozyme constructs were verified by DNA sequencing.

Ribozyme. Ribozymes were produced by *in vitro* transcription in a 50 µl reaction using linearized recombinant plasmid DNA as template (5 µg) in the presence of 27 U RNAGuard, 80 mM HEPES–KOH, pH 7.5, 24 mM $MgCl_2$, 2 mM spermidine, 40 mM DTT, 4 mM of each NTP, 0.01 U yeast pyrophosphatase and 25 mg purified T7 RNA polymerase at 37°C. After 3 h of incubation, 5 U DNase I (RNase-free) was added and the reaction incubated at 37°C for a further 30 min. The reaction mixtures were extracted with one volume phenol:chloroform (1:1), and fractionated by denaturing 20% polyacrylamide gel electrophoresis (PAGE, 19:1 ratio of acrylamide to bisacrylamide) using buffer containing 45 mM Tris-borate, pH 7.5, 7 M urea and 1 mM EDTA. The reaction products were visualized by UV shadowing, and the band corresponding to the ribozyme cut out. The transcripts were eluted from these gel slices overnight at 4°C in a solution containing 0.1% SDS and 0.5 M ammonium acetate, and were precipitated by the addition of 0.1 vol 3 M sodium acetate, pH 5.2, and 2.2 vol of absolute ethanol. Transcript quantities were determined by spectrophotometry at 260 nm.

Substrate. Deoxyoligonucleotides (500 pmol) harboring the substrate (Fig. 1) and the T7 promoter sequences were denatured by heating at 95°C for 5 min in a 20 µl solution containing 10 mM Tris–HCl, pH 7.5, 10 mM $MgCl_2$, 50 mM KCl, and allowed to slowly cool to 37°C. The *in vitro* transcriptions were carried out using the resulting partial duplex as template under the same conditions as those of ribozyme, and the substrate was purified and recovered as described above.

DNA/RNA mixed polymers. Substrates having a deoxyribose substituted for a ribose at one or two positions were chemically synthesized using an automated oligonucleotide synthesizer (Keck Biotechnology Resource Laboratory, Yale University), and then deprotected and purified as described previously (18). The resulting RNA mixed substrates were purified by PAGE and the corresponding bands excised and eluted as described above.

End-labeling of RNA

Purified transcripts (40 pmol) were dephosphorylated in a 20 µl reaction mixture containing 200 mM Tris–HCl, pH 8.0, 10 U RNAGuard and 0.2 U calf intestine alkaline phosphatase. The mixture was incubated at 37°C for 30 min, then extracted twice with 1 vol phenol:chloroform (1:1), ethanol precipitated, washed twice with 70% ethanol and dried. Dephosphorylated transcripts (5 pmol) were end-labeled with T4 polynucleotide kinase in the presence of 3.6 pmol [γ-^{32}P]ATP (6000 Ci/mmol) according to the manufacturer's recommended protocol. The reactions were stopped by the addition of 5 µl of formamide dye mixture (95% formamide, 10 mM EDTA, 0.05% bromophenol blue and 0.05% xylene cyanol), and fractionated on 20% PAGE gels. The labeled transcripts were eluted as described above, passed through a Sephadex G-50 spun column and stored at –20°C until used.

Metal ion-induced cleavage

Trace amounts (~0.01 pmol) of 5' end-labeled ribozyme were resuspended in 3 µl H_2O and then preincubated at 95°C for 2 min in either the presence or the absence of SdC4. After cooling on ice for 2 min, the mixtures were equilibrated at

37°C for 5 min. The cleavage reactions were initiated by adding 250 mM CHES–NaOH, pH 9.5 (1 µl) and 50 mM $MgCl_2$ (1 µl) and reaction incubating at 37°C for 2 h. The experimental conditions for cations other than Mg^{2+} are indicated in the legend to Table 2. The reactions were stopped by adding 50 mM EDTA, pH 8.0 (1 µl), and the resulting products ethanol precipitated, washed twice with 70% ethanol, air dried and dissolved in 6 µl of XC stop solution (95% formamide, 10 mM EDTA, 0.05% xylene cyanol) prior to fractionation on either 8 or 10% PAGE gels. In order to identify the cleavage sites, the reaction products and an RNA ladder produced by alkaline hydrolysis were fractionated on either 8 or 10% PAGE gels. The resulting gels were dried and exposed to an X-ray film and/or a PhosphorImager (Molecular Dynamics) screen when quantification was required.

Ribozyme cleavage activity

Under single turnover conditions, trace amounts of end-labeled synthetic substrate (<1 nM) were mixed with 200 nM of ribozyme in 20 µl of 50 mM Tris–HCl pH 7.9 solution. The mixtures were heated at 65°C for 2 min, and then cooled on ice for 2 min prior to preincubating at 37°C for 5 min. Following this preincubation, the cleavage reactions were initiated by the addition of divalent cations to a final concentration of 10 mM, and were followed for up to 6 h or until the endpoint of cleavage was reached. Aliquots of 2 µl were removed at various time intervals and mixed with 8 µl of an ice-cold solution containing 95% formamide, 10 mM EDTA, 0.05% bromophenol blue and xylene cyanol. Reaction products were resolved on 20% PAGE gels and the dried gels exposed to PhosphorImager screens. Radioactivity was quantified using the ImageQuant software in order to determine the fraction of substrate cleaved at each time point. The pseudo-first-order rate constants were obtained from non-linear least-square fitting of the data to the equation: cleaved yield $(\%P_t) = EP_0(1 - e^{-kt})$.

Nuclease mapping

Trace amounts (~0.01 pmol) of 5' end-labeled ribozyme were successively incubated for 2 min at 95°C, 2 min on ice and 5 min at 37°C in a 4 µl mixture containing 20 mM Tris–HCl pH 8.0, 4 mM $MgCl_2$ and 40 mM NH_4Cl. Either RNase T_1 (1 U) or RNase T_2 (0.5 U) was then added, and the mixtures incubated at 37°C for various durations. The reactions were quenched by the addition of 5 µl of XC stop solution (97% formamide, 10 mM EDTA and 0.02% xylene cyanol), and the cleavage positions analyzed as described in the previous section.

RESULTS AND DISCUSSION

Magnesium ion-induced cleavage in free ribozymes

The metal ion-induced cleavage approach was used to identify backbone phosphates involved in the coordination of magnesium ions within a *delta* ribozyme. The magnesium-induced cleavage patterns of 5' end-labeled ribozyme are shown in Figure 2. In the absence of metal ion the phosphodiester backbone remains intact (lane 3), while the presence of 10 mM magnesium ion promotes hydrolysis at several positions on the ribozyme in the absence of any substrate (lane 4). The P3 stem-loop (C_9–C_{16} and U_{19}), the P1 region (C_{20}–U_{26}) and the 5' part of both the J1/4 (G_{27}) and the J4/2 junctions (C_{47}–G_{51})

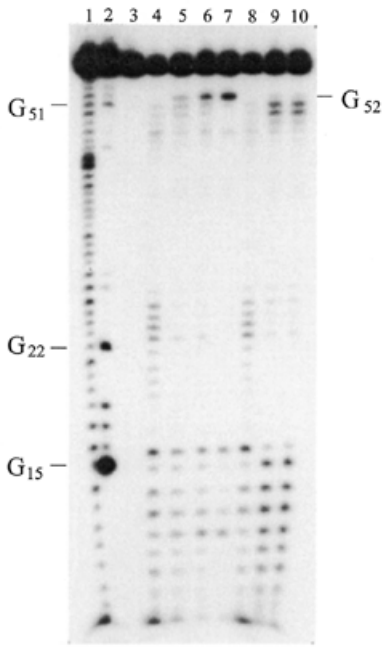

Figure 2. Magnesium-induced cleavage with various substrates. The end-labeled ribozyme was incubated alone without (lane 3) or with 10 mM magnesium (lane 4). The remaining lanes contain the ribozme, Mg^{2+} and the following substrates: SdC4 (lane 5), SalI (lane 6), P2 product (lane 7), unrelated sequence CCGACCU (lane 8), SU_8C (lane 9) and Sd4-SU_8C (lane 10). Alkaline hydrolysis (lane 1) and RNase T_1 hydrolysis (lane 2) of the end-labeled ribozyme were performed in order to determine the location of the metal ion-induced cleavage products (Materials and Methods). The locations of the RNase T_1 major cuts are indicated on the left, while the location of G_{52} is indicated on the right.

were all moderately hydrolyzed. All single-stranded regions were partially or entirely hydrolyzed with the exception of the L4 loop. This stable tetraloop has been reported to be resistant to lead hydrolysis (19). Since the tetraloop is not hydrolyzed by lead, one possible explanation is that the C-UUCG-G tetraloop displays an intrinsic resistance to magnesium-induced cleavage. A *delta* ribozyme with the reverse form of L4 loop (i.e. G-GCUU-C, see Fig. 1 inset), which is known for its relative instability (6) and for having similar kinetic parameters for cleavage of the 11 nt long substrate (5), showed similar magnesium-induced cleavage patterns with the exception that the phosphodiester backbone of the L4 loop was also hydrolyzed (data not shown). This difference indicates that the magnesium-induced cleavages in the L4 loop are local, involving different divalent metal ion(s) than those used in other single-stranded regions.

Magnesium-induced cleavage within the ribozyme–substrate complex

In order to study the magnesium-induced cleavage within the ribozyme–substrate complex, we initially used a non-cleavable substrate analog (SdC4). This analog has a deoxyribose substituted for the ribose at position 4, and was reported to act as a competitive inhibitor with a K_I similar to the K_M for the all RNA-substrate (5). In order to assure that that all molecules of ribozyme were bound (i.e. no free ribozyme), an excess of SdC4 was used. We detected some changes in the cleavage

products as compared to those obtained with the free ribozyme (Fig. 2, lane 5). First, the phosphodiester backbone connecting G_{52}, which is located at the bottom of the P2 stem, was hydrolyzed in the ribozyme–analog complex. Second, the region spanning the P1 stem (U_{19}–U_{26}) was cleaved substantially less than in the free ribozyme (compare lanes 4 and 5). Increasing the SdC4 concentration resulted in the detection of a larger quantity of the G_{52} cleavage product, while the hydrolysis in the P1 region decreased. Similar observations were detected with the ribozyme possessing the reverse L4 loop. In the presence of an excess of an unrelated substrate (lane 8), the cleavage pattern was similar to that seen when no analog was present (i.e. compare lanes 4 and 8). Thus, the formation of the P1 stem, which corresponds to the ribozyme–substrate complex, alters the induced cleavage pattern. In order to verify whether or not the cleavage pattern in the presence of the SdC4 analog was specific to this uncleavable substrate, similar experiments were performed with an excess of the all RNA-substrate (Sall) (lane 6). In the presence of the all RNA-substrate, the cleavage pattern of the ribozyme was similar to that obtained with SdC4 (lane 5); but, somewhat surprisingly, the G_{52} cleavage product was even more prevalent. The sole difference between Sall and SdC4 is the presence of the 2'-OH at the cleavage site, resulting in cleavable and uncleavable molecules, respectively. This single change seems to have a noticeable effect on the G_{52} cleavage product, even though to date there has been no evidence to indicate a proximity of the bottom of the P2 stem to the cleavage site of ribozymes of either polarity (1,7,20,21). The ribose at the scissile bond may therefore be indirectly involved in G_{52} cleavage product formation. Furthermore, since under the experimental conditions Sall could be catalytically cleaved by the ribozyme, the higher intensity of the G_{52} cleavage product with Sall might be the result of either the replacement of the 2'OH by 2'H or the presence of newly formed cleavage products. The ribozyme–product complex could be more flexible than the ribozyme–substrate complex, and consequently, the metal ion binding site is more accessible than in the ribozyme–analog complex. In order to verify this notion, experiments replacing either Sall or SdC4 with an equal amount of P2 product (the 3'-end product) were performed. Slightly higher G_{52} product levels were observed, indicating that the presence of a P1 stem is sufficient to yield G_{52} product, regardless of the presence or absence of sequence upstream of the cleavage site (Fig. 2, lane 7).

The kinetic and thermodynamic values obtained in mutational studies of the middle nucleotides of the P1 stem suggest that the binding and active sites of the *delta* ribozyme are uniquely formed (17). First, the substrate and the ribozyme are engaged in the formation of the P1 stem, which may contain a weak hydrogen bond(s) or bulge. Second, a tertiary interaction involving the base moieties in the middle of the P1 stem (positions 8 and 23 in the substrate and the ribozyme, respectively) is likely to play a role in defining the chemical environment of the active site. Therefore, we wondered whether or not the magnesium-induced cleavage was specifically related to one of these steps. The all RNA-substrate used above included a U at position 8, which base pairs with the A at position 23 of the ribozyme. We have previously demonstrated that the SU_8C substrate is able to bind to the ribozyme with an affinity similar to that of the native substrate (SU_8), even though a mismatch is present in the middle of the P1 stem, but that the resulting complex is completely inactive (16,17). We investigated the behavior of this particular substrate under metal ion-induced cleavage conditions (lane 9). As compared to the metal ion-induced cleavage of the ribozyme in the absence of substrate (lane 4), the presence of the SU_8C substrate results in the P1 region being hydrolyzed to a lesser extent, while the L3–P3 region (C_9–G_{15}) seemed to be hydrolyzed to a slightly greater extent (compare lanes 4 and 9). More importantly, the G_{52} cleavage product is no longer observed, while the A_{50} and the G_{51} cleavage products are now detected, although at reduced levels. The presence of an SU_8C analog harboring a deoxy nucleotide at position 4 resulted in a cleavage pattern (lane 10) closely resembling that obtained with the all RNA SU_8C mutant (lane 9). These results indicate that the P1 stem was formed, but that the difference observed at the level of the L3 loop may suggest that the complex differed in comparison to that formed with the Sall substrate. Furthermore, the absence of any G_{52} cleavage product indicates that the presence of a single mutation (U for C) generating a mismatch in the middle of the P1 stem is sufficient to cause reorganization of the binding site at the bottom of the P2 stem. Thus, the magnesium ion that hydrolyzed at G_{52} appears to be involved in the catalytic activity of the *delta* ribozyme, and not to be required for P1 stem formation.

It has been proposed that following formation of the P1 stem (i.e. ribozyme–substrate complex, RzS) an essential conformational transition is required for formation of the active ternary ribozyme–substrate complex (RzS') (5). If G_{52} is part of a magnesium-binding pocket, the presence of the metal ion in this pocket may be involved in this conformational transition. Position 8 of the substrate strongly influences its cleavability, but not its affinity for the ribozyme (17). We determined the influence of position 8 of the substrate on the appearance of the G_{52} cleavage product using ribozyme/substrate pairs for which the kinetic and thermodynamic parameters are known (Table 1). Under single turnover conditions, only the ribozyme–substrate complex in which the middle position of the P1 stem was base paired exhibited catalytic behavior, albeit at different levels as shown by the kinetic parameters. In contrast, a ribozyme in the presence of a non-cognate substrate which does not allow formation of a base pair in the middle of the P1 stem, exhibited no catalytic activity. In the presence of their respective cognate substrates (i.e. those forming a perfectly matched P1 stem), magnesium-induced cleavage of these ribozymes showed cleavage at G_{52}, although at different levels (Table 1). In contrast, the presence of a non-cognate substrate resulted in no G_{52} cleavage product under similar conditions for the same ribozymes (Table 1). For the complex involving a non-cognate substrate, increasing the $MgCl_2$ concentration did not permit recovery of the cleavage at G_{52}. Together, these results suggest that position S_8 must be conventionally base paired for G_{52} cleavage to occur. Furthermore, taking into consideration that the non-cognate substrates bind to the ribozymes with the same affinity as the cognate substrates, clearly the production of the G_{52} cleavage product is associated with the formation of an active ternary complex. The data reported in Table 1 were used for a comparative analysis of the kinetic parameters and the relative levels of G_{52} cleavage. The relative levels of induced cleavage at G_{52} varied directly with the apparent second-order rate constants ($k_2/K_{M'}$), and reciprocally

Table 1. Correlation between catalytic activity and the formation of the G_{52} cleavage product of each ribozyme–substrate pair

Ribozyme–substrate	k_2/K_M ($min^{-1}\,\mu M^{-1}$)[a]	K_{Mg} (mM)[a]	Relative levels of G_{52} cleavage product
Rz_{WT}-S_{WT}	19	2.2 ± 1.0	+++
Rz_{WT}-SU_8C	n.a.	n.a.	–
$RzA_{23}U$-SU_8A	76	1.9 ± 1.2	+++++
$RzA_{23}U$-SU_8C	n.a.	n.a.	–
$RzA_{23}G$-SU_8C	4	5.8 ± 1.0	+

[a]The k_2/K_M and K_{Mg} values are from (17). The relative levels of the G_{52} cleavage product (i.e. number of plus symbols) were determined by comparing the data of the various complexes.
n.a., not applicable.

with the concentration of magnesium at half-maximal velocity (K_{Mg}).

A collection of the RNA/DNA mixed substrates in which a single ribonucleotide was substituted for a deoxyribonucleotide at each position of the 11mer was synthesized (data not shown). Under single turnover conditions, all substrates were cleaved by the *delta* ribozyme at a level ranging from one equivalent to the native substrate to one either 2-fold more or 2-fold less. The variability in activity seemed to result from differences in the binding between the substrate and the ribozyme, caused by the presence of RNA/DNA heteroduplex in the P1 stem. With the exception of the nucleotide adjacent to the cleavage site, no 2'-OH in the substrate contributes to the cleavage. In the presence of all of these RNA/DNA mixed substrates, the magnesium-induced cleavage of the ribozyme yielded the G_{52} product. Together, these results indicate that none of the 2'-OH groups of the substrate contribute to the metal ion coordinate site involved in the bottom of the P2 stem.

Dependence of cleavage at G_{52} on the presence of a catalytically inactive ribozyme

The dependence of cleavage at G_{52} on the presence of a catalytically inactive ribozyme was also investigated (Fig. 3). We have previously shown that replacement of cytosine by adenosine at position 47 of the ribozyme (i.e. $RzC_{47}A$) renders it catalytically inactive (5). Magnesium-induced cleavage experiments using both 5' end-labeled $RzC_{47}A$ mutant ribozyme (lane 7) and wild type ribozyme (lane 3) in the absence of metal ion produced no cleavage product. The presence of 10 mM magnesium resulted in slightly different cleavage patterns (lanes 4 and 8). The $RzC_{47}A$ J4/2 junction seems to be hydrolyzed to a lesser extent, while its P4–L4 region is hydrolyzed to a greater extent than is observed with the Mg^{2+}-induced cleavage of the active ribozyme. The presence of the substrate analog (SdC4) changed the induced cleavage pattern of the active wild type ribozyme (lane 5), but had only little effect on that of the inactive $RzC_{47}A$ ribozyme (lane 9). The analog seems to cause a slight increase in the U_{48} cleavage product and a diminished amount of cleavage in the 5' part of the P1 region (C_{20}–G_{22}) of the mutant ribozyme, indicating a structural change. The 3' part of the P1 region (A_{23}–U_{26}) is still hydrolyzed, suggesting that the P1 stem structure is slightly different from the one formed in the active ribozyme (compare lanes 5 and 9). Finally, the cleavage at position G_{52} was not observed to occur with $RzC_{47}A$. Subsequent investigation of whether or not the presence of SalI could restore cleavage at G_{52} revealed that the induced

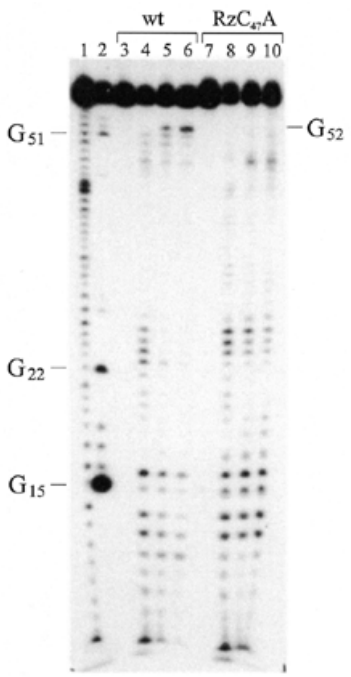

Figure 3. Magnesium-induced cleavage of an inactive ribozyme. Active (wild type) or inactive ($RzC_{47}A$) end-labeled ribozymes, respectively, were incubated in the absence of any substrate without (lanes 3 and 7) or with 10 mM magnesium (lanes 4 and 8), or with the substrates SdC4 (lanes 5 and 9) and SalI (lanes 6 and 10) in the presence of Mg^{2+}. Alkaline hydrolysis (lane 1) and RNase T_1 hydrolysis (lane 2) of the end-labeled ribozyme were performed in order to determine the location of the metal ion-induced cleavage products (Materials and Methods). The locations of the RNase T_1 major cuts are indicated on the left, while the location of G_{52} is indicated on the right.

cleavage of $RzC_{47}A$-SalI (lane 10) yielded a pattern similar to that obtained with the SdC4-analog. The 3' part of the P1 region was still hydrolyzed, and no G_{52} cleavage product was observed. Thus, the G_{52}-induced cleavage product is: (i) dependent on the presence of a conventional base pair at Rz_{23}-S_8; and (ii) is not observed in the presence of the $C_{47}A$ inactive ribozyme.

Magnesium- versus lead-induced cleavage

Lead ions have not been shown to support the catalytic activity of *delta* ribozyme (7; Table 2). In order to learn more about this

difference, we performed lead-induced cleavage experiments with the wild type ribozyme in either the presence or the absence of the SdC4-analog at neutral pH. In both cases, the lead-induced cleavage patterns were similar, except that the P1 stem was hydrolyzed to a lesser extent in the presence of the SdC4-analog. As compared to the magnesium-induced cleavage pattern the lead preferentially hydrolyzed the J4/2 junction, and the cleavage was observed regardless of whether or not the SdC4-analog was present. More importantly, the presence of the SdC4-analog did not allow one to observe hydrolysis at G_{52} (Table 2). These results agree with those from the lead-induced cleavage of a self-cleaved form of the genomic *delta* ribozyme (7). The efficiency of the lead-induced cleavage at these sites was substantially reduced in the presence of increasing amounts of $MgCl_2$ in the pre-incubation mixture, suggesting that these nucleotides may be at, or very near, a divalent cation binding site(s) (7). It is reasonable to believe that lead is an inactive ion because it does not support the formation of an active ribozyme complex, and consequently it produces a different cleavage pattern in the region near the bottom of the P2 stem. However, this hypothesis does not rule out the possibility that the difference in the cleavage patterns is caused by the intrinsic characteristic of these divalent cations. The magnesium ion (a 'hard' metal ion) tends to bind preferentially to oxygen ligands and phosphates, while the lead ion (a 'soft' metal ion) interacts preferentially with the aromatic nitrogen atoms of the nucleic acid bases (13).

Table 2. Correlation between the observed rate (k_{obs}) and the induced cleavage at positions A_{50}, G_{51} and G_{52} for several cations

Cation species	k_{obs} (min^{-1})	Induced cleavage positions		
		A_{50}	G_{51}	G_{52}
Mg^{2+}	0.21	–	–	+
Ca^{2+}	0.38	+	+	–
Mn^{2+}	0.06	+	–	–
Pb^{2+}	n.a.	–	–	–
Tb^{3+}	n.a.	–	–	–
Zn^{2+}	n.a.	–	–	–
Cd^{2+}	n.a.	–	–	–

Plus and minus symbols indicate the appearance or not, respectively, of induced cleavage products derived from end-labeled ribozymes when the SdC4-analog is present, as compared when it is absent. Mg^{2+} (10 mM), Ca^{2+} (10 mM), Mn^{2+} (10 mM), Zn^{2+} (5 mM) and Cd^{2+} (5 mM) were used at 37°C, while Pb^{2+} (4 mM) and Tb^{3+} (5 mM) were used at 25°C. The incubation time was optimized for each cation.
n.a., not applicable.

Several cations were evaluated for their ability to both support catalytic activity and to produce different induced cleavage patterns in the upper portion of the J4/2 junction (including the G_{52}) in the presence of the SdC4-analog as compared to in its absence (Table 2). Calcium and manganese support *delta* ribozyme activity, although at different levels. These cations showed different cleavage patterns in the J4/2 junction as compared to magnesium. For example, magnesium resulted in G_{52} cleavage, while calcium yielded cleavage at A_{50} and G_{51} solely in the presence of SdC4. These differences are

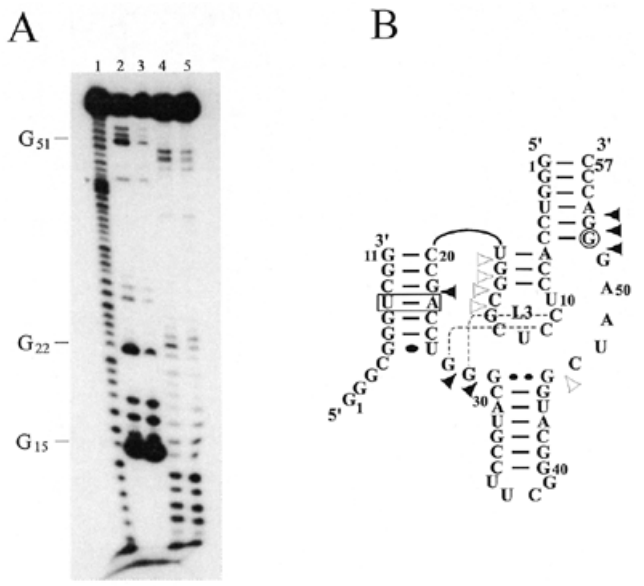

Figure 4. Nuclease mapping of a *trans*-acting *delta* ribozyme. (**A**) RNase T_1 and RNase T_2 probing, respectively, were performed on the end-labeled ribozyme in either the absence (lanes 2 and 4) or the presence of 1 μM SdC4 (lanes 3 and 5). Alkaline hydrolysis (lane 1) of the end-labeled ribozyme was performed in order to determine the location of the metal ion-induced cleavage products (Materials and Methods). The locations of the RNase T_1 major cuts are indicated on the left. (**B**) Summary of RNase T_1 probing. Filled or empty arrows represent a decrease or an equivalent level of RNase T_1 activity upon formation of the P1 stem, respectively. The rectangle indicates the mutated RzA_{23}-SU_8 base pair, and the circle indicates the G_{52} metal ion-induced cleavage product.

most probably caused by the different characteristics of the cations. More importantly, the presence of SdC4 yielded some differences in the cleavage pattern. We also examined several divalent cations that do not support the *delta* ribozyme catalytic activity (Table 2). Regardless of the presence or absence of the SdC4-analog none of these cations produced a different cleavage pattern in the J4/2 junction. Thus, cations which support catalytic activity show different ion-induced cleavage patterns in the presence of SdC4 (as compared to in its absence) while those that do not support the enzymatic process gave similar patterns irrespective of the presence or absence of the analog. These results suggest that the formation of the metal ion coordination site near the upper portion of the J4/2 junction is related to the formation of an active ternary complex, and discredit the hypothesis that a general charge screening of metal cations stabilizes the polyanionic phosphate backbone.

Nuclease mapping

Ribonuclease mapping has frequently been used to determine the secondary structure of *delta* self-cleaved ribozymes. It has been reported that self-cleaved ribozymes of both polarities are folded into similar pseudoknot secondary structures (22–24). We have used a similar approach to investigate whether or not structural changes occur near the bottom of the P2 stem. Using RNase T_1, which specifically hydrolyzes the RNA phosphodiester backbone after an unpaired guanosine residue (Fig. 4A,

lane 2), we find the most frequently cleaved nucleotides to be located in the 3' part of P3 stem–loop (G_{15}–G_{18}), in the middle of the P1 stem (G_{22}), on the 3' part of J4/2 (G_{51}) and on the 3' side of the P2 stem (G_{52} and G_{53}). In addition, minor products were observed corresponding to the J1/4 junction (G_{27}, G_{28} and G_{29}), and to one of the predicted homopurine base-pairing guanosines (G_{46}) (25). Similar assays were performed in the presence of 1 μM SdC4 (Fig. 4A, lane 3). To ensure that all ribozyme molecules were complexed with SdC4, we performed a denaturation/renaturation step followed by an incubation at 37°C (Materials and Methods). These experiments showed that both the P3 stem–loop and G_{46} were equally accessible in both cases. However, the amounts of cleavage products generated from both the middle of the P1 stem and from the J1/4 junction were reduced in the presence of SdC4. Recently, a new base paired region (P1.1) has been observed in a self-cleaved form of the genomic ribozyme (4). In our construction, this is represented by the potential formation of the base pairs G_{27}:C_{12} and G_{28}:C_{11}. The reduction in the amount of cleavage products detected in J1/4 upon the formation of the P1 stem could be attributed to formation of the P1.1 stem. This hypothesis would imply that the P1.1 helix would form concomitantly with formation of the P1 stem. Unexpectedly, the amounts of cleavage products generated from the stretch of guanosines located near the bottom of the P2 stem were greatly reduced. These results imply that a local rearrangement is occurring at the bottom of the P2 stem when the P1 helix is formed. The RNase T_1 probing results are summarized in Figure 4B. As described above, some structural rearrangements seem to occur upon the formation of the P1 stem (filled arrows in Fig. 4B).

Nuclease mapping experiments using RNase T_2, a non-specific endoribonuclease which hydrolyzes the phosphodiester bonds of single-stranded RNA preferentially on the 3' side of A residues, were also performed (Fig. 4A, lane 4). The predominant cleavage products derived from the L3 loop (C_9–C_{14}), the middle of the P1 stem (A_{23}) and the middle part of the J4/2 junction (A_{49} and A_{50}). Minor products were detected in the 3' part of the P3 stem–loop (G_{15}–U_{19}), in the P1 stem (C_{20}–G_{22} and C_{24}–C_{25}), in the L4 loop (C_{38}) and in the J4/2 junction (U_{48}). Similar experiments were also conducted in the presence of 1 μM SdC4 (lane 5). The relative fractions of cleavage products detected were equal throughout the molecule except for the middle parts of both the P1 region (A_{23}) and J4/2 junction (A_{48} and A_{49}), which were cleaved substantially less. Together, the ribonuclease T_1 and T_2 mapping results support a structural change involving at least the 3' part of the J4/2 and the bottom of the P2 stem upon the formation of the P1 helix. This correlates with the formation of the metal ion coordination site as shown by generation of the G_{52} product in magnesium-induced cleavage.

Is the specific binding of Mg^{2+} required for either folding or catalysis?

Divalent metal ions play an indispensable role in the folding and/or active site chemistry of *delta* ribozyme (8). The best way to correlate metal binding site and folding of a given RNA is to do a minimal disruption of this binding site by a single nucleotide mutation and to characterize the resulting molecule. Here we correlate the detection of a metal binding site with both the catalytic activity and the proper folding of the RNA. We determined the ability of several ribozyme–substrate complexes to generate G_{52} cleavage product under magnesium-induced cleavage conditions. In all cases, catalytic ability correlated with detection of the G_{52} cleavage product. This magnesium binding site can be detected and modulated by the nature of the Rz_{23}-S_8 base pair, and is not observed in the presence of the C_{47}A inactive ribozyme. This method does not conclusively determine whether or not Mg^{2+} is required for the folding and/or catalysis of the *delta* ribozyme, but it does show that both events are intimately associated. In addition, RNase mapping detected a reorganization of at least the 3' part of the J4/2 junction and the bottom of the P2 stem upon the formation of the P1 helix. This correlates with the formation of the metal ion coordination site as shown by generation of the G_{52} product in the magnesium ion-induced cleavage experiments.

A previous study of the antibiotic inhibition of a *delta* ribozyme suggested that both neomycin and magnesium likely displace lead ion(s), raising the hypothesis that *delta* ribozymes do indeed have a metal ion associated at some coordination site(s) (7). Furthermore, it has been postulated that a *delta* ribozyme composed of three RNA oligomer strands is bound by three Mg^{2+} ions, and that a conformational change is induced by Mg^{2+} ion titration (as monitored by CD spectra; 20). In addition, it was demonstrated by chemical probing that structural re-arrangements might occur in genomic *delta* ribozymes in the presence of Mg^{2+} ions, particularly ones that induce tertiary contacts (26). These studies clearly show that *delta* ribozymes interact with metal ions, and that structural changes can be monitored in different ways.

Several studies, including Fe(II)–EDTA protection assays and cross-linking experiments, suggested that *cis*- and *trans*-acting *delta* ribozymes of both genomic and antigenomic polarities have similar global tertiary structures, and that only subtle differences exist between the different forms (21,24). Therefore, it is surprising that the crystal structure of a self-cleaved form of the genomic *delta* ribozyme did not show any tightly bound metal ions (4). To stimulate ribozyme crystal formation, the ribozyme was constructed so that it bound a small, basic protein while still being active. The crystal structure of this ribozyme appeared to be stabilized entirely by base-pairing, stacking, non-canonical base–backbone and back-bone–backbone interactions (4). In contrast to other studies (including this one), the absence of metal ion in the crystal structure can be explained in several ways: (i) we used a *trans*-acting system, while the crystal structure was obtained with a self-cleaved form that includes the J1/2 junction; and (ii) the crystal structure was obtained using the self-cleavage product which may not include the magnesium ion involved in the G_{52} cleavage. It is possible that the crystal structure of the *cis*-form product corresponds to that of the inactive *trans*-form observed with the C_{47}A-mutant or with non-cognate substrates. In the case of the lead-catalyzed specific cleavage of $tRNA^{Phe}$, structures of both the uncleaved and the cleaved RNA have been published (13). In the uncleaved structure, Pb^{2+} was observed to be bound with high frequency at the cleavage site. Once the tRNA has been cleaved, the Pb^{2+} dissociates, and is therefore not observed in the cleaved structure. A similar scenario appears plausible as an explanation for the lack of Mg^{2+} in the cleaved form of the *cis*-acting *delta* ribozyme.

In conclusion, we strongly believe that there is at least one magnesium ion coordination site present in a *trans*-acting form of the antigenomic *delta* ribozyme. This magnesium ion binding site can be detected and modulated by the nature of the

Rz_{23}-S_8 base pair, and is not observed in the presence of the $C_{47}A$ inactive ribozyme.

ACKNOWLEDGEMENTS

This work was supported by a grant from the Medical Research Council (MRC) of Canada to J.P.P. D.A.L. was the recipient of a doctoral fellowship from the Fonds de la Recherche en Santé du Québec (FRSQ). S.A. was the recipient of a postdoctoral fellowship from Natural Sciences and Engineering Research Council (NSERC) of Canada. J.P.P. is an MRC scholar.

REFERENCES

1. Been,M.D. and Wickham,G.S. (1997) *Eur. J. Biochem.*, **247**, 741–753.
2. Mercure,S., Lafontaine,D., Roy,G. and Perreault,J.P. (1997) *Médecine/ Science*, **13**, 662–667.
3. Perrotta,A.T. and Been,M.D. (1991) *Nature*, **350**, 434–436.
4. Ferré-D'Amaré,A.R., Zhou,K. and Doudna,J.A. (1998) *Nature*, **395**, 567–574.
5. Mercure,S., Lafontaine,D., Ananvoranich,S. and Perreault,J.P. (1998) *Biochemistry*, **37**, 16975–16982.
6. Varani,G. (1995) *Annu. Rev. Biophys. Biomol. Struct.*, **24**, 379–404.
7. Rogers,J., Chang,A.H., Ahsen,U.V., Schroeder,R. and Davies,J. (1996) *J. Mol. Biol.*, **259**, 916–925.
8. Murray,J.B., Seyhan,A.A., Walter,N.G., Burke,J.M. and Scott,W.G. (1998) *Chem. Biol.*, **5**, 587–595.
9. Sanger,H.L., Ramm,K., Domdey,H., Gross,H.J., Henco,K. and Riesner,D. (1979) *FEBS Lett.*, **99**, 117–122.
10. Gast,F.U., Kempe,D., Spieker,R.L. and Sanger,H.L. (1996) *J. Mol. Biol.*, **262**, 652–670.
11. Kazakov,S. and Altman,S. (1991) *Proc. Natl Acad. Sci. USA*, **88**, 9193–9197.
12. Streicher,B., Westhof,E. and Schroeder,R. (1996) *EMBO J.*, **15**, 2556–2564.
13. Pan,T., Long,D.M. and Uhlenbeck,O.C. (1993) In Gesteland,R.F. and Atkins,J.F. (eds), *The RNA World*. Cold Spring Harbor Laboratory Press, Cold Spring Harbor, NY, pp. 371–302.
14. Zawadzki,V. and Gross,H.J. (1991) *Nucleic Acids Res.*, **19**, 1948.
15. Davanoo,P., Rosenberg,A.H., Dunn,J.J. and Studier,F.W. (1984) *Proc. Natl Acad. Sci. USA*, **81**, 2035–2039.
16. Ananvoranich,S. and Perreault,J.P. (1998) *J. Biol. Chem.*, **273**, 13182–13188.
17. Ananvoranich,S., Lafontaine,D.A. and Perreault,J.P. (1999) *Nucleic Acids Res.*, **27**, 1473–1479.
18. Perreault,J.P. and Altman,S. (1992) *J. Mol. Biol.*, **226**, 399–409.
19. Ciesiolka,J., Michalowski,D., Wrzesinski,J., Krajewski,J. and Krzyzosiak,W.J. (1998) *J. Mol. Biol.*, **275**, 211–220.
20. Sakamoto,T., Tanaka,Y., Kuwabara,T., Kim,M.H., Kurihara,Y., Katahira,M. and Uesugi,S. (1997) *J. Biochem. (Tokyo)*, **121**, 1123–1128.
21. Rosenstein,S.R. and Been,M.D. (1996) *Biochemistry*, **35**, 11403–11413.
22. Lee,C.B., Lai,Y.C., Ping,Y.H., Huang,Z.S., Lin,J.Y. and Wu,H.N. (1996) *Biochemistry*, **35**, 12303–12312.
23. Been,M.D., Perrotta,A.T. and Rosenstein,S.P. (1992) *Biochemistry*, **31**, 11843–11852.
24. Rosenstein,S.P. and Been,M.D. (1991) *Nucleic Acids Res.*, **19**, 5409–5416.
25. Been,M.D. and Perrotta,A.T. (1995) *RNA*, **1**, 1061–1070.
26. Kumar,P.K.R., Taira,K. and Nishikawa,S. (1994) *Biochemistry*, **33**, 583–592.